Protein Science (1997), 6:2397–2408. Cambridge University Press. Printed in the USA.

Characterization of a helix-loop-helix (EF hand) motif of silver hake parvalbumin isoform B

SANDRA P. REVETT,[1] GINA KING,[2] JEFFREY SHABANOWITZ,[2] DONALD F. HUNT,[2] KARI L. HARTMAN,[3] THOMAS M. LAUE,[3] AND DONALD J. NELSON[1]

[1]Gustaf H. Carlson School of Chemistry, Clark University, Worcester, Massachusetts 01610
[2]Department of Chemistry, University of Virginia, Charlottesville, Virginia 22901
[3]Department of Biochemistry, University of New Hampshire, Durham, New Hampshire 03824

(RECEIVED March 18, 1997; ACCEPTED July 7, 1997)

Abstract

Parvalbumins are a class of calcium-binding proteins characterized by the presence of several helix-loop-helix (EF-hand) motifs. It is suspected that these proteins evolved via intragene duplication from a single EF-hand. Silver hake parvalbumin (SHPV) consists of three EF-type helix-loop-helix regions, two of which have the ability to bind calcium. The three helix-loop-helix motifs are designated AB, CD, and EF, respectively. In this study, native silver hake parvalbumin isoform B (SHPV-B) has been sequenced by mass spectrometry. The sequence indicates that this parvalbumin is a β-lineage parvalbumin. SHPV-B was cleaved into two major fragments, consisting of the ABCD and EF regions of the native protein. The 33-amino acid EF fragment (residues 76–108), containing one of the calcium ion binding sites in native SHPV-B, has been isolated and studied for its structural characteristics, ability to bind divalent and trivalent cations, and for its propensity to undergo metal ion-induced self-association. The presence of Ca^{2+} does not induce significant secondary structure in the EF fragment. However, NMR and CD results indicate significant secondary structure promotion in the EF fragment in the presence of the higher charge–density trivalent cations. Sedimentation equilibrium analysis results show that the EF fragment exists in a monomer–dimer equilibrium when complexed with La^{3+}.

Keywords: calcium-binding protein; EF-hand; helix-loop-helix; parvalbumin; silver hake

Calcium-binding proteins are a class of proteins with important functions in enzyme activation, muscle contraction, and cell growth. A common structural characteristic of these proteins is the EF-hand, a helix-loop-helix motif formed by a sequence of about 30 amino acids (Kretsinger & Nockolds, 1973; Kretsinger, 1975; Kretsinger & Nelson, 1976). Members of this homologous group of proteins contain from two to eight repeats of the helix-loop-helix motif, with the EF domains generally occurring in pairs. The fact that EF-hands naturally occur in pairs implies that this domain partnering plays an important role in protein stabilization and function. It is suspected that, through intragene duplication, these proteins evolved from a single approximately 40-amino acid ancestral calcium-binding peptide (Kretsinger, 1972). This intragene duplication likely led to an elongated protein with greater stability and specificity than the ancestral protein. About one-third of the EF-hand domains in this superfamily of proteins do not bind calcium (Kawasaki & Kretsinger, 1994).

Parvalbumins, a subfamily of EF-hand calcium-binding proteins, have three EF-hand repeats, two of which are paired and bind calcium tightly. The N-terminal EF-hand noncalcium-binding domain forms a cap that covers the hydrophobic surface formed by the paired C-terminal calcium-binding domains. Within the parvalbumin subfamily, two distinct phylogenic lineages (α and β) have been identified. Beta parvalbumins are usually shorter by one residue and have lower pI values (pI $<$ 5.0) than α-parvalbumins (pI $>$ 5.0). Common to all known parvalbumin sequences is an invariant arginine at residue 75, near the beginning of the carboxyl-terminal EF domain. X-ray crystallography and NMR data reveal a strong structural homology between members of the parvalbumin subfamily. For example, pike 4.10 and carp 4.25 (Kumar et al., 1990; Declercq et al., 1991), both β-parvalbumins, are very similar in tertiary structure.

SHPV-B is a 108-amino acid β-parvalbumin isolated from white muscle of silver hake (*Merluccius bilinearis*). This approximately 11.4-kDa protein is the major of three isoforms purified from this source (Zhang et al., 1990). The three-dimensional structure of carp parvalbumin has been determined by X-ray crystallography and provides a good model for comparison with SHPV-B based on sequential homology, particularly in the EF region. The conserved Arg 75 residue offers an ideal proteolytic site for clostripain (Gilles et al., 1979) because it is located at the beginning of the carboxyl-terminal helix-loop-helix domain. A second advantageous feature

Reprint requests to: Donald J. Nelson, Gustaf H. Carlson School of Chemistry, Clark University, Worcester, Massachusetts 01610; e-mail: dnelson@vax.clarku.edu.

of SHPV-B is the presence of a single tryptophan residue, which permits experimental exploration of structure–function relationships by several methods, such as fluorescence and UV spectroscopy.

Proteolytic protein fragments and designed synthetic peptides have become useful tools in revealing binding mechanisms and folding characteristics of native proteins. The formation of stable tertiary structure by relatively short synthetic polypeptides (23 amino acids) in aqueous solution even in the absence of disulfide bonds or metals has been demonstrated (Shoemaker et al., 1987; Struthers et al., 1996). Achievement of stable structure for some protein fragments, however, requires formation of a dimeric complex (Williams & Moreton, 1988; Roongta et al., 1989; Prat Gay & Fersht, 1994; Prat Gay et al., 1994). The complexes formed in this manner by protein fragments frequently adopt native-like structure (Kippen et al., 1994; Rico et al., 1994).

The study of synthetic analogues and chemically or proteolytically generated peptides representing binding sites in EF-hand calcium-binding proteins has provided important insight into the structural stability and binding characteristics of this class of proteins. Studies of isolated EF-hand calcium-binding sites, however, indicate that Ca^{2+} is commonly required to induce native-like structure (Reid et al., 1981; Gariépy et al., 1982, 1983, 1985; Borin et al., 1985) and fragment complexation (Drabikowski et al., 1982; Gariepy et al., 1982; Shaw et al., 1990, 1991b, 1992a, 1992b, 1992c; Shaw & Sykes, 1996; Kay et al., 1991; Permyakov et al., 1991; Durussel et al., 1993). For example, NMR data have shown that a 34-residue peptide representing the high-affinity calcium-binding site III of troponin C (TnC) undergoes a random coil to helix-loop-helix shift and dimerization in the presence of calcium (Shaw et al., 1990, 1991a, 1991b). The formation of calcium-induced homodimeric complexes has also been observed in a peptide corresponding to site IV of TnC (Kay et al., 1991) and in EF-hand peptides of calbindin D_{9K} (Finn et al., 1992; Linse et al., 1993) and *Nereis* sarcoplasmic calcium-binding protein (Durussel et al., 1993). In the presence of calcium, single-site EF-hand peptides also form heterodimeric complexes (Shaw et al., 1992a, 1992c; Shaw & Sykes, 1996). In the case of TnC, the EF-hand heterodimers have greater stability than homodimers (Shaw et al., 1994). Cooperative stabilization derived from the pairing of calcium-binding sites may account for the observed formation of dimeric complexes from helix-loop-helix fragments (Monera et al., 1992; Shaw et al., 1994; Shaw & Sykes, 1996). Formation of dimeric complexes by EF-hand peptides demonstrates the importance of domain pairing in protein stability and metal ion binding. This concept is consistent with data showing that paired calcium-binding domains in native proteins, such as parvalbumin and TnC, are stable at temperatures of about 90 °C (Filimonov et al., 1978; Tsalkova & Privalov, 1985; Williams et al., 1986; Cox et al., 1990). For example, Williams et al. (1986) have reported a T_m of approximately 87 °C in CD studies of Ca^{2+}-bound rat α-parvalbumin.

Stabilization by domain pairing is supported by studies of one- and two-site domain fragments of TnC. A peptide containing calcium-binding sites III and IV exhibits a Ca^{2+} affinity that is 200-fold stronger than that of a peptide containing site III alone (Reid et al., 1981).

Although calcium-binding protein fragments apparently require Ca^{2+} to form stable structures, Ca^{2+} affinity is generally much weaker than in the native protein (Derancourt et al., 1978; Tsuji & Kaiser, 1991). Homodimers formed from helix-loop-helix peptides also have significantly weaker affinities for Ca^{2+} (Reid, 1990; Kay et al., 1991; Shaw et al., 1991; Tsuji & Kaiser, 1991; Linse et al., 1993). Calcium affinity is enhanced in heterodimers formed from the EF-hands of two different proteins or different regions of the same protein. However, Ca^{2+} affinities of heterodimers are much weaker than those of intact proteins (Permyakov et al., 1991; Finn et al., 1992; George et al., 1993).

In aqueous solution, trivalent lanthanides, such as Tb^{3+} and La^{3+}, form complexes with six-coordinate ionic radii comparable to Ca^{2+}. Thus, lanthanides are useful probes for investigating the role of Ca^{2+} in proteins and have been used extensively to examine the metal affinities of parvalbumins (Nelson et al., 1977; Miller et al., 1980; Lee & Sykes, 1983; Drakenberg et al., 1985; Lee et al., 1985; Ragg et al., 1986; Eberspach et al., 1988; Zhang & Nelson, 1992). Recent studies have used lanthanides to investigate the kinetics and mechanism of Ca^{2+} binding in EF-hand proteins (Renner et al., 1993; Drake & Falke, 1996).

The purpose of the present study is to determine by mass spectrometry the sequence of SHPV-B (in order to place this parvalbumin isoform in its appropriate phylogenic lineage and to verify the position of the single arginine residue), to isolate the EF calcium-binding site of SHPV-B by digestion with the arginine-specific enzyme, clostripain, to study and compare the fragments' ability to assume native-like structure and function in the presence of both the biological metal ion, calcium, and trivalent lanthanide probe ions, and to assess the propensity of the EF fragment to undergo metal ion-induced self-association.

Results and discussion

Sequencing and characterization of native SHPV-B

Mass spectrometry data indicate a molecular weight of 11,357 ± 3.5 amu for the intact protein. Figures 1 and 2, respectively, show the proteolytic digestion map and the sequence of SHPV-B determined by mass spectrometry. The primary sequence of silver hake parvalbumin displays a high degree of homology with that of β-parvalbumins from other closely related fish species (Fig. 2). The calcium-binding (EF-hand) region of the protein is highly conserved. The EF calcium-binding sites in parvalbumins whose structures have been determined have been shown to be solvent-exposed. This is consistent with the observation that digestion of the whole protein for short periods of time (10–20 min) yielded mostly digestion products from the EF region. Also, peptides from the EF region were among the most concentrated products following longer enzymatic digestions. This observation supports the view that the EF region in SHPV-B is solvent-exposed, consistent with crystal structure data on other parvalbumins. Solvent accessibility of the EF site is a well-known conserved feature of parvalbumins (Strynadka & James, 1989; Falke et al., 1994).

Unusual characteristics of SHPV-B include a high content of alanine residues and a single tryptophan residue at position 102. Of the approximately 40 known parvalbumin sequences, only two others, cod and whiting, have a single tryptophan residue located at this position. As in other fish parvalbumins, SHPV-B has a highly conserved single arginine residue at position 75, preceding the carboxyl-terminal helix-loop-helix motif of the protein.

Results of isoelectric focusing experiments indicate a pI of 4.2 for native SHPV-B. This relatively low pI, along with primary sequence characteristics of the protein, place SHPV-B in the β phylogenic class of parvalbumins. For example, the Cys 18, Asp 61, and the 108-amino acid length of the protein are characteristic of β-parvalbumins (Kretsinger, 1980).

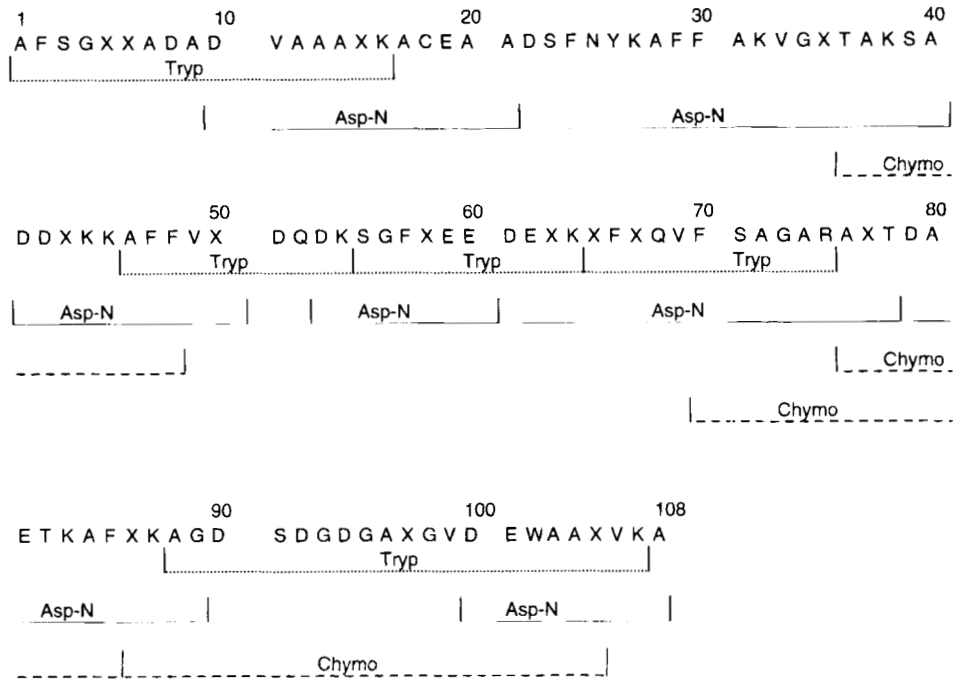

Fig. 1. Proteolytic map of SHPV-B showing fragments generated for sequencing by mass spectrometry. Ile and Leu are shown as X because these residues cannot be distinguished from one another due to their identical residue weight.

Based on results of BLAST, basic alignment search tool (Altschul et al., 1990), for comparison of known primary structures, SHPV-B shares a high sequence homology with carp parvalbumin. The two parvalbumins have 89 identically located residues.

NMR spectroscopy of native and apoSHPV-B

One-dimensional ^{1}H NMR of native SHPV-B (Fig. 3, spectrum C) shows that the protein is rich in secondary structure. The dispersed sharp peaks in the upfield and downfield regions of the native protein spectrum are evidence of side-chain and backbone amide protons in unique structural environments. The single upfield-shifted methyl peak has been attributed to a γ-methyl resonance band of Val 106 (Padilla et al., 1988).

The 1D ^{1}H NMR spectrum of random coil peptides commonly shows a lack of dispersion in chemical shift (for a given proton type, e.g., Ala methyl proton) throughout the spectrum. Removal of Ca^{2+} from SHPV-B appears to cause sweeping chemical-shift changes throughout the NMR spectrum that include loss of peak dispersion. In the apoprotein (Fig. 3, spectra A and B), broad peaks in the upfield and downfield regions and loss of downfield-shifted backbone amide proton resonances indicate that significant loss of structure occurs following release of calcium. The single downfield resonance at about 10 ppm in Figure 3, spectrum B (apoSHPV-B in 90% H_2O) is characteristic of the Trp 102 indole NH proton. A high alanine content is indicated by the large upfield resonance band in the methyl region of the spectra.

Isolation and characterization of the SHPV-B EF fragment

Digestion of apoSHPV-B

Native SHPV-B was found to be resistant to enzymatic cleavage at Arg 75. Attempts to cleave native SHPV-B at Arg 75 with both trypsin and clostripain were unsuccessful (data not shown). Removal of Ca^{2+} from the native protein renders the site susceptible to proteolysis, because enzymatic digestion of the apoprotein resulted in cleavage at the desired position. The elution profile of the Sephadex G-50 chromatography of the digestion mixture (Fig. 4) shows three major peaks, suggesting that three fragments were generated by clostripain digestion of the apoprotein.

UV spectroscopy of the SHPV-B fragments

The pool of larger fragments (Fig. 4, Pool 1) generated in the clostripain digestion of apoSHPV-B is expected to contain the ABCD fragment (residues 1–75 of the native protein) and possibly, undigested apoprotein. UV analysis of Pool 1 supports the presence of peptides with a high content of phenylalanine and no tryptophan.

UV spectra of pools of the two smaller SHPV-B fragments, represented by Pools 2 and 3 in Figure 4, are identical. The UV spectra of Pool 1 in Figure 4 differs significantly from that of Pools 2 and 3. A strong peak at approximately 290 nm in the UV spectrum of Pool 2 is consistent with the presence of tryptophan. Multiple peaks in the 250–270-nm region of the spectrum of Pool 1 indicate the presence of several phenylalanine residues. The absence of similar multiple peaks in the 250–270-nm region of the UV spectrum of Pools 2 and 3 is evidence of a relatively low phenylalanine content for these protein fragments. Also, the broad hump at ~280 nm in the Pool 1 spectrum indicates the presence of tyrosine.

Amino acid analysis of the SHPV-B fragments

HPLC analysis showed that Pool 2 (Fig. 4) contains a single peptide. Comparison of amino acid analysis with the known amino acid content of SHPV-B residues 76–108 (Table 1) demonstrates that the Pool 2 peptide has an amino acid content consistent with

	10	20	30	40
Pike (pI 4.10)*	S F A G L K D A D	V A A A L A A C S A	A D S F K H K E F F	A K V G L A S K S L
Carp (pI 4.25)	A F A G V L N D A D	I A A A L E A C K A	A D S F N H K A F F	A K V G L T S K S A
Whiting (pI 4.50)	A F A G I L A D A D	A C A A V K A C E A	A D S F S Y K A F F	A K C G L S G K S A
Cod (pI 4.40)**	A F K G I L S N A D	I K A A E A A C F K	E G S F D E D G F Y	A K V G L D A F S A
E. Hake (pI 4.36)	A F A G I L A D A D	I T A A L A A C K A	E G S F K H G E F F	T K I G L K G K S A
S. Hake (pI 4.20)***	**A F S G I L A D A D**	**V A A A L K A C E A**	**A D S F N Y K A F F**	**A K V G L T A K S A**

	50	60	70	80
Pike (pI 4.10)*	D D V K K A F Y V I	D Q D K S G F I E E	D E L K L F L Q N F	S P S A R A L T D A
Carp (pI 4.25)	D D V K K A F A I I	D Q D K S G F I E E	D E L K L F L Q N F	K A D A R A L T D G
Whiting (pI 4.50)	D D I K K A F V F I	D Q D K S G F I E E	D E L K L F L Q V F	K A G A R A L T D A
Cod (pI 4.40)	D E L K K L F K I A	D E D K E G F I E E	D E L F L F L I A F	A A D L R A L T D A
E. Hake (pI 4.36)	A D I K K V F G I I	D Q D K S D F V E E	D E L K L F L Q N F	S A G A R A L T D A
S. Hake (pI 4.20)	**D D I K K A F F V I**	**D Q D K S G F I E E**	**D E L K L F L Q V F**	**S A G A R A L T D A**

	90	100	110
Pike (pI 4.10)*	E T K A F L A D G D	K D G D G M I G V D	E F A A M I K A
Carp (pI 4.25)	E T K T F L K A G D	S D G D G K I G V D	E F T A L V K A
Whiting (pI 4.50)	E T K A F L K A G D	S D G D G A I G V E	E W V A L V K A
Cod (pI 4.40)	E T K A F L K A G D	S D G D G K I G V D	E F G A L V D K W G A K G
E. Hake (pI 4.36)	E T A T F L K A G D	S D G D G K I G V E	E F A A M V K G
S. Hake (pI 4.20)	**E T K A F L K A G D**	**S D G D G A I G V D**	**E W A A L V K A**

Fig. 2. Amino acid sequences of SHPV-B and other fish β-parvalbumins. References: pike, pI 4.10 (Gerday, 1976); carp, pI 4.25 (Coffee & Bradshaw, 1973); whiting, pI 4.50 (Joassin & Gerday, 1977); cod, pI 4.40 (Elsayed & Bennich, 1975); E. hake, pI 4.36 (Capony et al., 1973). * Pike sequence of 107 amino acids has been offset by one residue to best illustrate homology with other β-parvalbumins. ** Subsequent sequencing of the tryptophan-containing tryptic fragment of cod yielded the following sequence: A^{88}GDSDGGDAIGVDEW^{102}AVLVK^{107} (Hutnik et al., 1990). *** Ile and Leu residues, indistinguishable by mass spectrometry, were assigned by comparison with homologous parvalbumin sequences.

this region of the protein. Residues 76–108 of SHPV-B constitute the EF (the third helix-loop-helix) region of the native protein. Although amino acid analysis is unable to verify the presence of Trp, a downfield-shifted peak characteristic of the indole NH of Trp is present in the 1D and 2D ^{1}H NMR spectra of the Pool 2 fragment.

HPLC and amino acid analysis of Pool 3 indicate that clostripain, which has up to a 500:1 preference for cleavage of Arg over

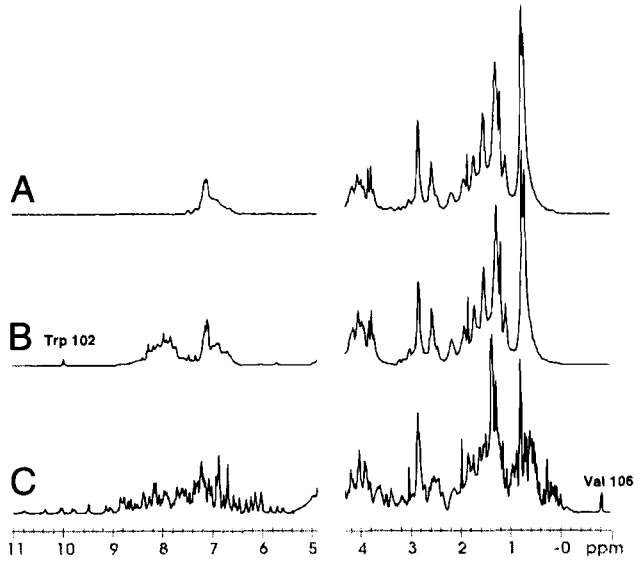

Fig. 3. One-dimensional ^{1}H NMR spectra (at 500 MHz) of (**A**) apoSHPV-B, 0.55 mM in 100% D_2O, pH 7.7, (**B**) apoSHPV-B, 0.68 mM in 10% D_2O, 90% H_2O, pH 6.48; and (**C**) native SHPV-B, 1.32 mM in 10% D_2O, 90% H_2O, pH 6.55.

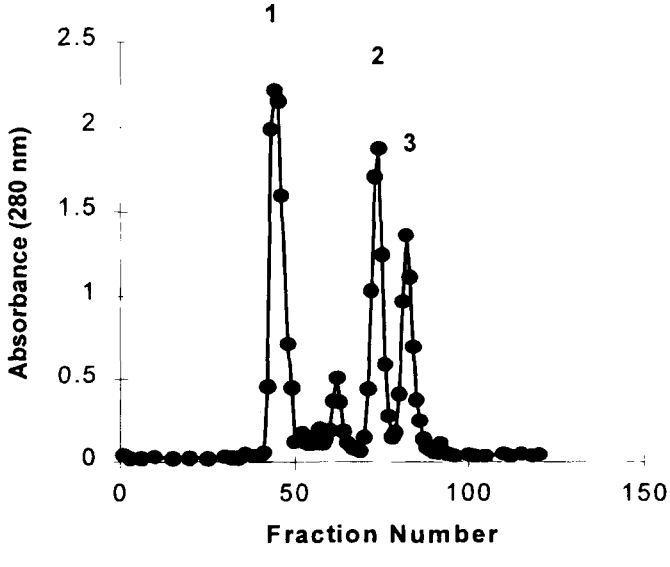

Fig. 4. Sephadex G-50 gel filtration elution profile for clostripain digestion of apoSHPV-B. Column (1.5 cm × 170 cm) was equilibrated with 0.1 M NH_4HCO_3 and eluted at 6.8 mL/h. Fractions in correspondingly labeled peaks were pooled to form Pool 1, Pool 2, and Pool 3.

Table 1. *Amino acid analysis of sample of Pool 1 from Sephadex G-50 column*

Amino acid	Composition	
	Expected[a]	Experimental
Asp	5	5.3
Ser	1	1.1
Glu	2	2.0
Gly	4	4.0
Thr	2	1.9
Ala	8	7.6
Val	2	2.1
Lys	3	2.7
Ile	1	0.9
Leu	3	2.7
Phe	1	0.9
Trp	1	—

[a]Expected amino acid content based on native SHPV-B sequence for residues 76–108.

Lys residues (Mitchell & Harrington, 1968), also cleaves apoSHPV-B at Lys 83. Pool 3, therefore, consists of a fragment representing residues 84–108 of the native protein.

The third major fragment (Fig. 4, Pool 1) generated in the clostripain digest of apoSHPV-B likely consists of the ABCD fragment (residues 1–75 of the native protein) and possibly, a small amount of undigested apoprotein. UV analysis of Pool 1 indicates the presence of peptides with a high content of phenylalanine and little or no tryptophan.

The minor proteolytic fragment eluting between Pools 1 and 2 has not been characterized.

Mass spectrometry of the EF fragment

Three charge states (+3, +4, and +5) for the EF fragment were present in the mass spectra, and a parent mass of 3,307.2 ± 0.5 amu was calculated using these values. These results are in close agreement with a computer-generated molecular weight of 3,306.2 (unprotonated) for the EF fragment.

CD of native SHPV-B and the EF fragment

The CD spectrum of native SHPV-B (Fig. 5A, spectrum b) is typical of a protein with significant α-helical content (~31%), as evidenced by the minima in ellipticity, [θ], at 208 and 222 nm. The α-helical content of the apoprotein (Fig. 5A, spectrum a) was about 21%, indicating a loss of approximately one-third of the helical structure of the native protein upon removal of Ca^{2+}. The CD spectra of the EF fragment alone and in the presence of a twofold molar excess of calcium (Fig. 5B, spectra a and b, respectively) are very similar, both indicating a relatively low degree of α-helicity (~10%). Calcium apparently cannot induce the required octahedral ordering of the loop coordinating ligands, which may well be a prerequisite for the induction of α-helical coiling of the flanking peptide region. [It was expected that the CD spectrum in the presence of Ca^{2+} would indicate higher α-helicity, because Ca^{2+} caused significant changes in the 1D ^{1}H NMR spectrum of the EF fragment. Specifically, the 1D ^{1}H NMR spectrum of the EF fragment in the presence of Ca^{2+} (Fig. 7, spectrum A, following) revealed significant methyl resonance dispersion and general resonance line broadening. The dispersal of the peptide proton NMR signals in the presence of Ca^{2+} may be the result of nonspecific Ca^{2+} binding or Ca^{2+}-induced aggregation. The absence of α-helical structure in the CD sample is consistent with very weak or nonspecific binding of Ca^{2+} to the EF fragment.]

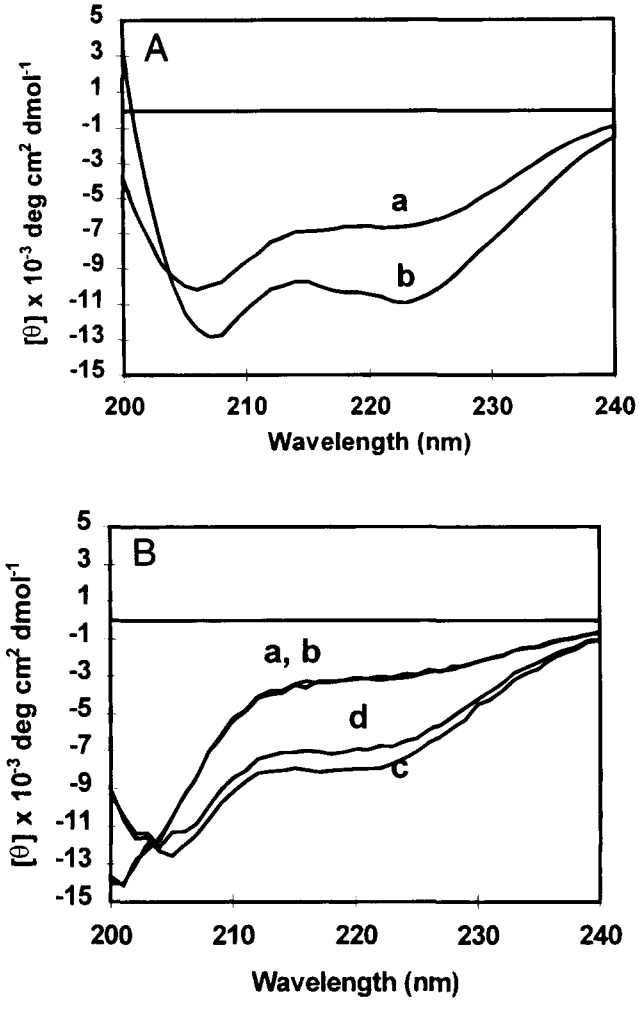

Fig. 5. CD spectra of apoSHPV-B, native SHPV-B, and SHPV-B EF fragment under a variety of ionic and solvent conditions. All samples are in 2 mM HEPES, 50 mM KCl, pH 7.0. **A:** CD spectra of (a) apoSHPV-B and (b) native SHPV-B. **B:** CD spectra of (a) EF fragment and EF fragment with a twofold molar excess of (b) Ca^{2+} and (c) Tb^{3+} or (d) La^{3+}.

CD spectra of the EF fragment in the presence of Tb^{3+} and La^{3+} (Fig. 5B, spectra c and d, respectively), commonly used trivalent lanthanide probes of calcium ion, proved to be very similar and indicative of a conformation with significant α-helical content (~24% and ~21%, respectively). Thus, in contrast to divalent calcium, the trivalent lanthanides, with their relatively high charge density, promote structure formation in the EF fragment.

Thermal and structural stability of the EF fragment–lanthanum complex is shown in Figure 6. The α-helical structure induced by the binding of La^{3+} is relatively stable up to 60 °C (Fig. 6, spectra b). Upon increasing the temperature of this sample to 80 °C, a relatively insignificant amount of α-helical structure (~4%) was lost (data not shown). The thermal stability of the La^{3+}-bound peptide is comparable to that of native parvalbumin, which, as stated previously, has been shown to retain secondary structure at

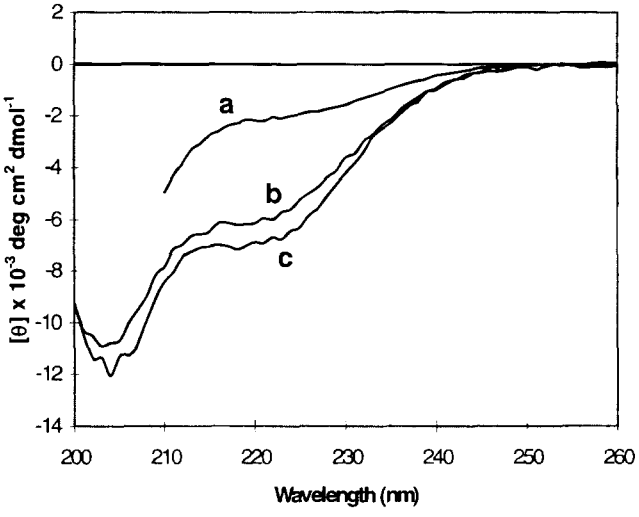

Fig. 6. CD spectra of 30 μM EF fragment with a twofold molar excess of La^{3+} in (a) 2.5 M guanidine HCl; (b) 2 mM HEPES, 50 mM KCl at 60 °C; and (c) 2 mM HEPES, 50 mM KCl at 25 °C.

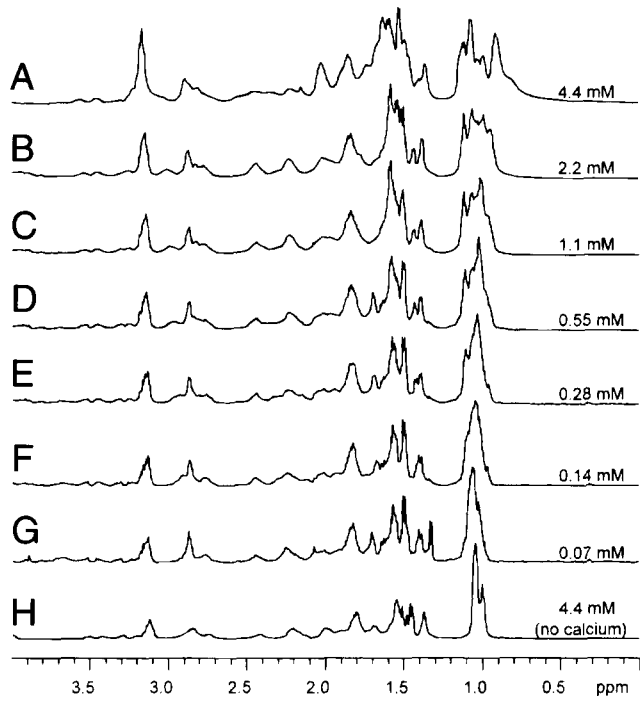

Fig. 7. One-dimensional ^1H NMR spectra (at 500 MHz) of a 1:2 mixture of EF fragment and Ca^{2+} as a function of peptide concentration. Spectra A–G have EF fragment concentrations of 4.4 mM, 2.2 mM, 1.1 mM, 0.55 mM, 0.28 mM, 0.14 mM, and 0.07 mM, respectively. Spectrum H corresponds to 4.4 mM EF fragment in the absence of Ca^{2+}. The pH of all samples was between 6.3 and 6.4.

temperatures approaching 90 °C. In the presence of 2.5 M GdmCl, however, a loss of α-helical conformation occurs (Fig. 6, spectrum a). Thus, it appears that GdmCl is an effective agent in unfolding the La^{3+}–EF fragment complex.

NMR spectroscopy of the EF fragment of SHPV-B

The 1D ^1H NMR spectrum of random coil peptides, as stated previously, usually shows a lack of dispersion in chemical shift throughout the spectrum. As evidenced in results of the dilution study of the EF fragment (Fig. 7), in the absence of Ca^{2+}, the NMR spectrum of the EF fragment has little dispersion of resonances, indicating the presence of random coil structure (Fig. 7, spectrum H). Similar NMR evidence of random coil structure has been obtained for calcium-free EF-hand analogues of TnC site III and site IV or mixtures of sites III and IV (Shaw et al., 1992a). Upon addition of Ca^{2+}, the upfield and downfield regions of the 1D ^1H NMR spectrum show significant changes in chemical shifts for the EF fragment (Fig. 7, spectrum A). Upfield methyl and methylene peaks are particularly broad and more dispersed in the presence of Ca^{2+}. Peaks in the amide region are also broadened upon addition of Ca^{2+}.

The 1D ^1H NMR spectra of successive dilutions of the EF fragment in the presence of a twofold molar excess of Ca^{2+} show a concentration-dependent change in chemical shifts (Fig. 7). As peptide concentration decreases, the upfield region of the spectrum of the EF fragment with Ca^{2+} (Fig. 7, spectra A–G) approaches that of the EF fragment in the absence of Ca^{2+} (Fig. 7, spectrum H). (Note that both spectra A and H in Figure 7 have a peptide concentration of 4.4 mM, but only the sample associated with spectrum A has Ca^{2+}.)

Removal of Ca^{2+} from the EF fragment by chelation with EDTA results in a 1D ^1H NMR spectrum that closely resembles that of the fragment prior to addition of Ca^{2+}. Broad methyl and methylene peaks in the spectrum of the EF fragment with Ca^{2+} collapse to fewer and narrower peaks upon removal of Ca^{2+}, demonstrating the reversibility of the effects of Ca^{2+} on the EF fragment.

As shown in Figure 7, addition of Ca^{2+} to the EF fragment results in significant changes in the 1D ^1H NMR spectrum. When the EF fragment was titrated with Ca^{2+}, the relatively narrow spectral lines in the Ca^{2+}-free peptide became increasingly broader and more dispersed as the Ca^{2+}:peptide ratio was increased from 0 to 20. In the 1D ^1H NMR spectra, methyl resonances in the Ca^{2+} titration of the EF fragment showed an increase in base width that continued beyond the addition of one molar equivalent of Ca^{2+} (relative to peptide) to the fragment solution. After the addition of 3.5 molar equivalents of Ca^{2+}, only slight changes occurred in the methyl peak region. This indicates that, although a major change in proton environments is apparently induced in the EF fragment by Ca^{2+}, the binding of Ca^{2+} to the fragment is likely weak and nonspecific.

To summarize the potential effects of Ca^{2+} on the EF fragment, 1D ^1H NMR spectra for the EF fragment in the presence and absence of Ca^{2+} and for the dilution experiment of the EF fragment with Ca^{2+} are consistent with a kinetic reaction order greater than 1, which would be the case if dimerization were occurring. This suggests the possibility of Ca^{2+}-induced dimerization or higher multimerization of the EF fragment. Ca^{2+}-induced dimerization is a commonly observed phenomenon in fragments of Ca^{2+}-binding proteins (Shaw et al., 1990, 1991a, 1991b; Kay et al., 1991; Permyakov et al., 1991). Although 1D ^1H NMR data are consistent with multimerization of the EF fragment in the presence of Ca^{2+}, the results of sedimentation equilibrium experiments (see following) do not support this. A more likely cause of the observed broadening of resonances for the EF fragment in the presence of Ca^{2+} is nonspecific binding of Ca^{2+} to the EF fragment. Nonspecific binding is also indicated by the stoichiometric data observed in the titration of the EF fragment with calcium and by the results

of CD experiments, which show that Ca^{2+} has no apparent effect on the amount of α-helix in the EF fragment. Although the EF fragment contains one of the two binding sites present in the native protein, the presence of five Asp and two Glu and over 30 carbonyl groups provide ample ligands for nonspecific binding of Ca^{2+}.

In marked contrast to the results obtained for Ca^{2+}, an analogous titration experiment with La^{3+} showed that significant changes in the methyl region occurred up to a 1:1 molar ratio of cation to peptide (Fig. 8). This 1:1 stoichiometry is evidence of site-specific binding to the single calcium-binding site in the EF fragment. Figure 9 summarizes the effects of Ca^{2+} and La^{3+} on the structure of the EF fragment. Similar stoichiometry has been observed in binding studies of tryptic fragments of TnC (Leavis et al., 1978; Drabikowski et al., 1982).

Not all EF-hand peptides exhibit 1:1 calcium stoichiometry. Unusual stoichiometry has been noted in calcium-binding studies of sites III and IV of TnC. Titration experiments in which changes in the 1D ^{1}H NMR, CD, or fluorescence spectrum were monitored as calcium was added to the peptide have indicated stoichiometries (Ca:peptide) ranging from 0.5 to 20 (Shaw et al., 1990, 1991a, 1992c; Kay et al., 1991).

The effect of La^{3+} on proton resonances of the EF fragment is especially apparent in the upfield portion of the 1D ^{1}H NMR spectra shown in Figure 10, spectrum A. In the presence of La^{3+}, upfield peaks become more dispersed, likely indicative of a higher degree of secondary structure in the La^{3+}-bound EF fragment. In the spectrum of the Ca^{2+}-bound EF fragment (Fig. 10, spectrum B), peaks are broader and less dispersed compared to those in the spectrum of the La^{3+}-bound EF fragment. This effect is also observed in the downfield region of the 1D ^{1}H NMR spectrum.

TOCSY β-proton region chemical-shift data for two unique hydrophobic aromatic residues in the EF fragment in the absence and presence of either Ca^{2+} or La^{3+} are listed in Table 2. These residues correspond to Phe 85 and Trp 102 in the native protein. In the TOCSY spectrum of the EF fragment in water, strong peaks for Phe 85 (7.90 ppm) and Trp 102 (7.96 ppm) are present. Duplicate sets of peaks that appear in the spectrum (at 7.12 ppm and 7.16 ppm, respectively) arise from ^{4}J coupling between the beta protons and ring protons of the aromatic side chains. Evidence of this unusual coupling is absent in the spectrum of EF fragment with Ca^{2+}. Ca^{2+} induces little change in the NH backbone or C_β chemical shifts of Trp 102. For Phe 85, however, the backbone NH resonance undergoes a downfield shift by almost 0.1 ppm and the C_β protons become degenerate.

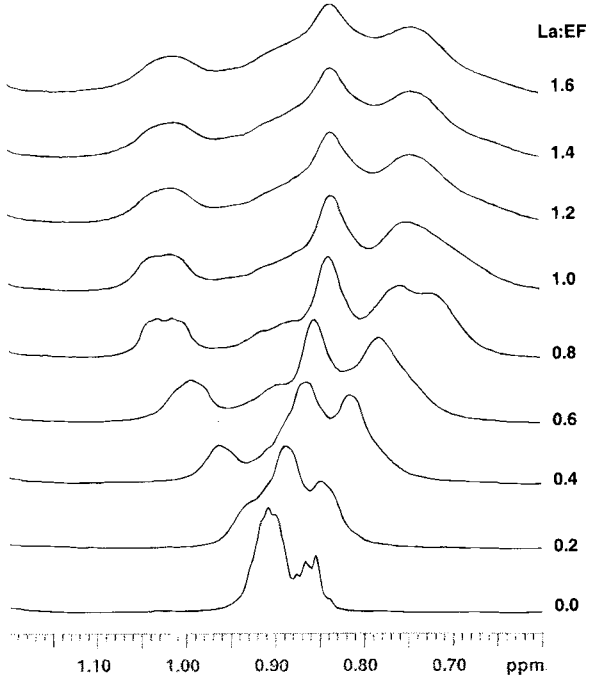

Fig. 8. Stacked plot of 1D ^{1}H NMR spectra (at 500 MHz) showing changes in the methyl region during La^{3+} titration of 2.6 mM EF fragment. Molar ratios of La^{3+} to fragment appear at right of spectra.

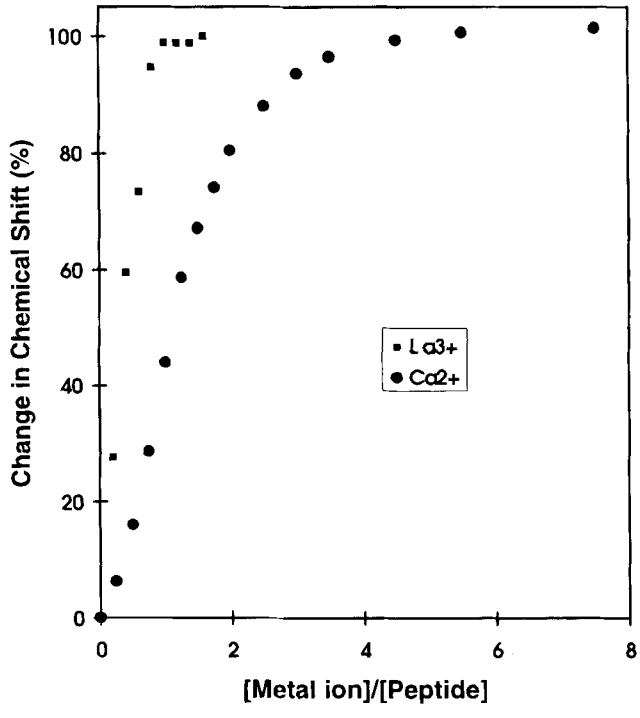

Fig. 9. Plot of percent change in chemical shift of upfield methyl peak in 1D ^{1}H NMR spectra (at 500 MHz) versus ratio of concentration of metal ion to EF fragment. Concentration of EF fragment was 2.6 mM for La^{3+} and 2.8 mM for Ca^{2+} titration.

La^{3+} causes the largest change in Trp 102 resonances. In the presence of La^{3+}, Trp 102 NH resonance shifts approximately 0.5 ppm upfield, whereas C_β proton chemical shifts move upfield by about 0.2 ppm and 0.25 ppm, respectively, relative to resonances of EF fragment in water. The Phe 85 NH resonance is affected less by this trivalent cation. Compared to backbone NH resonances for the peptide in the absence of cations, La^{3+} induces a nearly 0.1 ppm downfield shift in the Phe 85 NH resonance.

TOCSY ^{1}H NMR data are consistent with CD data, both indicating that the higher charge density metal ion (La^{3+} in the case of the NMR experiment) is most efficient in inducing structural change in the EF fragment.

Sedimentation equilibrium analysis of EF fragment of SHPV-B

The z-average molecular weight for the Ca^{2+}-bound EF fragment was 2,960 ± 100, and showed no concentration dependence, indicating that the EF fragment is monomeric under these condi-

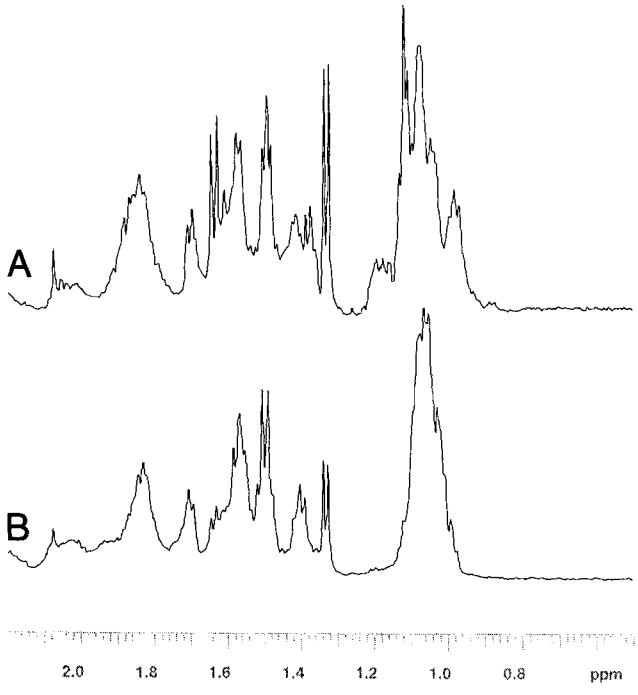

Fig. 10. Upfield region of 1D ^1H NMR spectra (at 500 MHz) of (**A**) 0.07 mM EF fragment in ~98% D_2O with twofold molar excess of La^{3+}, pH 6.1, and (**B**) 0.07 mM EF fragment in ~98% D_2O with twofold molar excess of Ca^{2+}, pH 6.4.

tions. The discrepancy between this molecular weight and that from mass spectrometry likely results from errors introduced by the use of a calculated partial specific volume. In the presence of La^{3+}, there was an increase in the z-average molecular weight as the peptide concentration increased, suggesting a mass-action equilibrium. A global analysis of the combined data from different loading concentrations and different rotor speeds reveals that the data fit best (RMS = 0.006 Å) to a model of an ideal monomer–dimer equilibrium with an apparent monomer molecular weight of 3,130 (2,990–3,280), a stoichiometry of assembly of 2.1 (1.9–2.3), and an association constant of 1,477 (1,252–1,720) 1/M, corresponding to an association energy of −17.8 (17.4–18.1) kJ/mol.

Table 2. *Chemical shifts (in ppm) of EF fragment aromatic residues corresponding to Phe 85 and Trp 102 of native SHPV-B*

	Phe 85		Trp 102	
Sample conditions	NH	$C_\beta H$	NH	$C_\beta H$
(A) H_2O	7.90	3.02, 2.93	7.96	3.24, 3.15
(B) Ca^{2+}	7.99	2.95	7.97	3.23, 3.14
(C) La^{3+}	7.99	3.01	7.51	3.05, 2.89

[a]Specific sample conditions were as follows: (A) 4.4 mM EF fragment in 10% D_2O, 90% H_2O, (B) 4.4 mM EF fragment in 10% D_2O, 90% H_2O with twofold molar excess of Ca^{2+}, and (C) 2 mM EF fragment in 10% D_2O, 90% H_2O with twofold molar excess of La^{3+}. The pH of samples was between 6.4 and 6.5 (pH 6.06 for La^{3+} sample). Peptide concentration was about 4.4 mM (2 mM for La^{3+} sample).

Models in which the stoichiometry of assembly was forced to higher values would not fit the data adequately. Models in which higher-order oligomers were included in the model did not improve the fit.

Conclusions

The amino acid sequence of the major parvalbumin isoform from silver hake (SHPV-B), determined by mass spectrometry, indicates that the protein has a β parvalbumin phylogenic lineage. The 108-amino acid length of the protein, the presence of cysteine and aspartic acid at positions 18 and 61, and a pI value of 4.2 are all consistent with this phylogenic placement. The sequence further indicates the presence of an arginine residue at position 75, as is the case for all parvalbumins whose sequences have been determined. The fortuitous location of this arginine residue has facilitated excision, using the arginine-specific cleavage agent clostripain, of the carboxyl-terminal helix-loop-helix (EF-hand) repeat unit.

The excised EF-hand, following confirmation of identity and assessment of purity by mass spectrometry, has been examined for its ability to undergo metal ion-induced structure induction. CD studies of aqueous solutions of the EF fragment (at micromolar concentrations) in the presence of the biological metal, Ca^{2+}, indicate little tendency to adopt secondary. In contrast, CD results on EF fragment solutions in the presence of trivalent lanthanides, such as La^{3+} and Tb^{3+}, clearly indicate structure induction. The higher charge density lanthanide ions apparently have the ability to interact with sufficient numbers of coordinating ligands and place them in an environment that is conducive for α-helical coiling of a significant portion of the EF fragment chain. The CD results, which support lanthanide ion-induced structuring of the EF fragment, are supported by the results of 1D and 2D ^1H NMR experiments performed on samples containing the EF fragment and the nonparamagnetic La^{3+} ion. It is not yet known if the precise constellation of lanthanide ion-coordinating ligands is similar to the coordination environment found around the Ca^{2+} ion in the native protein. Future NMR and X-ray crystallography experiments will be performed to address this question.

The CD experiments do not provide evidence for Ca^{2+} binding to the EF fragment. Because the CD studies provide no evidence for Ca^{2+} ion induction of helical structure *and* because the NMR and sedimentation equilibrium studies suggest nonspecific binding to the EF fragment, which exists as monomer in the presence of calcium, we conclude that the isolated EF fragment exhibits very weak Ca^{2+} binding affinity. Weak Ca^{2+} binding ($K_d = 3 \times 10^{-3}$ M) to the EF fragment of carp parvalbumin has been reported (Derancourt et al., 1978). Typical dissociation constants for native parvalbumins are approximately 2×10^{-7} M (Benzonana et al., 1972), representing 10,000-fold stronger binding of Ca^{2+} in the intact protein. At low peptide concentrations, however, trivalent lanthanide ions clearly induce structure in the EF fragment. In summary, CD and NMR results obtained on the EF fragment are not consistent with folding of the EF fragment *in the presence of* Ca^{2+} into a native-like structure with its requisite α-helical content. The isolated EF region is relatively unstructured and flexible in aqueous solvent and, consequently, requires a cation of higher charge density to induce structure.

An important finding of this study is that, in the presence of La^{3+} (but *not* Ca^{2+}), the SHPV-B EF fragment forms a dimer. Along with the apparent lack of site-specific binding of Ca^{2+} to the EF fragment, this observation provides strong evidence that the

behavior of the EF-hand of SHPV-B differs from that of other calcium-binding EF-hand proteins (e.g., TnC, calretinin, and NSCP), which typically have been observed to bind Ca^{2+} specifically and to form Ca^{2+}-induced dimers.

Further experiments should include NMR analysis of the tertiary structure of the dimeric La^{3+}-bound EF fragment to determine if the dimeric structure has native-like characteristics. It has been proposed that the driving force for protein fragment complementation is formation of a hydrophobic core (Shaw et al., 1991a). X-ray crystallography structures indicate that hydrophobic faces of amphiphilic helices in the second and third helix-loop-helix domains of carp parvalbumin, indeed, form a hydrophobic core. This may also be the case for SHPV-B.

Materials and methods

Materials

SHPV-B was purified by the method described by Pechère et al. (1971). Endoproteinase Asp-N (*Achromobacter lyticus*), chymotrypsin A_4 (sequencing grade), and bovine trypsin (sequencing grade) enzymes were purchased from Boehringer Manneheim (Indianapolis, Indiana). HPLC columns, RP-300 Aquapore (C_8 2.1 mm i.d. × 30 mm, 7 μm particles), OD-300 Aquapore (C_{18} 2.1 × 30 mm, 7 μm particles, 300 Å pore), RP-18 Spheri-5 (monofunctional C_{18} 2.1 × 30 mm, 5 μm particles, 80 Å pore), and BU-300 Aquapore (C_4 2.1 × 30 mm, 7 μm particles) were all purchased from Brownlee Labs, Rainin Instrument Company (Woburn, Massachusetts). All other chemicals used were reagent grade.

Methods

Sequencing and characterization of SHPV-B

Preparation of protein/peptides for mass spectrometry. Digestion of the native protein (0.50–2.00 nmol) was performed with trypsin, chymotrypsin, or endoproteinase Asp-N (1:50–1:100 enzyme:peptide, by weight). Tryptic and chymotryptic digestions were performed in 50 mM ammonium bicarbonate, pH 8.5, at 37 °C for 1–12 h. The endoproteinase Asp-N digestion was performed in 50 mM sodium phosphate buffer (dibasic and monobasic), pH 8.0, at 37 °C for 3.5 h. Following the incubation period, peptide mixtures were separated by reverse-phase HPLC. Fractions that represented peaks on the chromatogram were collected and prepared for sequencing by tandem mass spectrometry by lyophilizing the volume by half to remove the acetonitrile.

Purification of the intact protein and digestion fragments by reverse-phase HPLC was performed on an Applied Biosystems (Foster City, California) model 130A Separation System. Approximately 1 nmol of SHPV-B was purified using a BU-300 Aquapore reverse-phase column. Stock solutions (2–20 nmol/μL) of the protein were prepared directly by solubilizing the lyophilized powder in a 5% acetic acid solution. Carboxyamidation was not required, because amino acid analysis indicates that the protein contains only one cysteine. Peptide fragments (100–700 pmol in 5% acetic acid) were injected into either an OD-300 Brownlee column, RP 300 Aquapore column, BU-300 column, or a RP-18 Spheri-5 column. A 40-min linear gradient of 0–100% solvent B (60% acetonitrile, 0.085% TFA) in 0.1% TFA was employed at 200 μL/min. The amide backbone, which absorbs at 214 nm, was monitored using a 440 Absorbance Detector. Fractions representing individual peaks on the chromatogram were collected manually into 1.5-mL eppendorf tubes and acetonitrile was removed by vacuum centrifugation in preparation for tandem mass spectrometry.

Esterification of glutamic and aspartic acid side chains were performed by first depositing an aliquot from each HPLC fraction into siliconized microtubes. Peptides (40–500 pmol) were then lyophilized to dryness. A 3 M methanolic HCl reagent was prepared by adding 160 μL of acetyl chloride dropwise to 1 mL of anhydrous methanol with constant stirring for 5 min. A 30–40-μL aliquot of the reagent was added to the lyophilized peptide and the mixture was allowed to stand at room temperature for 90 min. After lyophilizing the solution to dryness, the esterified peptide was solubilized in 5% acetic acid.

N-Acetylations (on column) of the N-terminus and side chains of lysine residues were performed on microcapillary columns prior to analyzing peptides by tandem mass spectrometry. Acetylation reagents were prepared by adding 1 μL of acetic anhydride to 99 μL of 100–200 mM ammonium acetate, pH 8.5. The peptide was loaded onto the back of a Poros packed microcapillary column, as described later, and washed with deionized water for 5 min. The freshly prepared acetylation reagent was washed over the column for 11 min and the column was flushed with deionized water for 5 min prior to connection of the column to the HPLC. After washing the column for 3 min with solvent A (0.1% TFA), the gradient was started and the acetylated peptide analyzed.

Matrix assisted laser desorption ionization time of flight (MALDI-TOF) mass spectrometry of SHPV-B. Approximately 1 pmol of purified parvalbumin in a saturated matrix solution of alpha-cyano-4-hydroxy-cinnamic-acid in 50% acetonitrile was loaded onto the TOF stainless steel probe tip and pulsed with a nitrogen laser at 337 nm. Protein standards of insulin (5,733 MW) and myoglobin (16,961 MW) were co-added to the matrix solution for internal calibration. The instrument, constructed in-house (Department of Chemistry, University of Virginia), includes a 350-Hz digital oscilloscope where data was collected and then processed with modified Lasermat software (Finnigan, San Jose, California).

Electrospray ionization and tandem mass spectrometry of proteolytic peptides. The mass spectra of the HPLC-purified digestion products of SHPV-B were recorded on a Finnigan TSQ-700 and TSQ-70μ triple quadrupole mass spectrometer equipped with a microcapillary reverse-phase column and an electrospray ion source. The first quadrupole (Q1), which has both rf and dc current applied to it, was generally set to scan *m/z* (mass to charge) values of 300–1,400. The transmitted ions were detected by a conversion dynode electron multiplier, which operates at 15 keV. Mass spectra in a given *m/z* range were acquired every 1.5 s and mass spectra were summed over one or several chromatographic peaks. Charge states were analyzed in main beam mode and the most abundant ion for each peptide was determined.

After the most abundant ion for each species was determined, more peptide sample was loaded onto the column and the ion with the most abundant mass to charge ratio was selected in the first quadrupole. In the second quadrupole, the ion was collisionally activated by bombardment with argon gas (2–3 millitorr). In this experiment, the third quadrupole (Q3) was set for a scan range starting at 50 *m/z* and having an upper limit based on the mass to charge of the parent ion. A collisionally activated dissociation (CAD) spectrum, displayed as relative ion abundance versus *m/z*, was obtained and the sequence of the peptide was deduced from the data.

Isoelectric focusing of SHPV-B. The pI of SHPV-B was determined on a Bio-Rad model 111 IEF Minicell apparatus. Polyacrylamide gels were prepared and run per Bio-Rad manual procedures. In gel preparation, 40% ampholytes (Bio-Lyte 3/10) ranging in pH from 3 to 10 were used. A 1.5-μL sample of SHPV-B (4.6 mg/mL) and of standards (pI 3.6–9.6) were applied to the gel and the gel was run at 450 V for 2 h. Fixing and destaining were performed using Bio-Rad reagents and procedures.

NMR spectroscopy of native and apoSHPV-B. ^{1}H NMR spectra were recorded on a Varian Unity 500 MHz NMR spectrometer and processed on a Sun Microsystems computer. The native protein sample was prepared by dissolving 12 mg of SHPV-B in 800 μL of a 90% H_2O/10% D_2O solution (1.32 mM in SHPV-B) containing a 2:1 molar excess of Ca^{2+}. For the apoSHPV-B sample in water, 5.4 mg of apoprotein were dissolved in 700 μL of 10% D_2O/90% H_2O (v/v) solution, resulting in a 0.68 mM protein solution. The final apoprotein concentration was 0.34 mM. When necessary, the pH was adjusted using 0.2 M NaOH. All sample solutions were between pH 6.5 and 6.6. An external reference of tetramethylsilane (TMS) was used.

NMR spectra were acquired at 25 °C, collecting 256 scans with a spectral width of 6,500 Hz. Water suppression was achieved by presaturation during the 50-ms relaxation delay.

Isolation and study of SHPV-B EF fragment

Preparation of apoSHPV-B. ApoSHPV-B was prepared by EDTA extraction of Ca^{2+} from native SHPV-B. An EDTA solution was prepared by dissolving EDTA in double-deionized H_2O and adjusting solution to pH 6 with 2 M NaOH. SHPV-B was dissolved in double-deionized H_2O and EDTA solution added until a 10:1 molar excess of EDTA:SHPV-B was achieved. The pH of the protein solution was adjusted to 8.2 and allowed to stand at 4 °C overnight. The apoSHPV-B solution was transferred to a dialysis bag having a 6,000 to 8,000 molecular weight cut-off and dialyzed first versus 1 mM EDTA, pH 8.0, and then exhaustively versus 0.1 M NH_4HCO_3, pH 8.0. The apoSHPV-B was recovered from solution by lyophilization and stored at −20 °C. Complete removal of EDTA, a strong deactivator of clostripain (Mitchell & Harrington, 1968), was confirmed by 1D ^{1}H NMR analysis of the apoSHPV-B on a 500 MHz Varian NMR spectrometer.

Digestion of apoSHPV-B. Clostripain obtained from Sigma (catalog number C-7403) was activated by a 3-h incubation of 3 mg of enzyme in 0.8 mL of 2.5 mM DTT, 125 mM sodium phosphate, pH 7.7 buffer. Approximately 100 mg of apoSHPV-B were added to the activated clostripain solution along with 1 mL of 4 M urea and 0.2 mL of double-deionized H_2O. Digestion was allowed to proceed for 4 h. Throughout the digestion period, the enzyme/protein solution was maintained at about pH 7.7 by addition of 0.1 M NaOH.

Immediately following digestion, the enzyme/protein solution was applied to a Sephadex G-50-50 chromatography column (170 cm × 1.5 cm) equilibrated with 0.1 M NH_4HCO_3. The column was eluted with 0.1 M NH_4HCO_3 at a rate of 6.8 mL/h. Fractions were collected at 20-min intervals and examined for digestion products by UV spectroscopy. Spectra (240–300 nm) were acquired on an HP 8452A diode array spectrophotometer.

UV spectroscopy of SHPV-B fragments. UV spectra were taken at room temperature on an IBM 9420 UV-Vis spectrophotometer using a 1-cm pathlength quartz cuvette. The instrument was blanked on the same buffer as in the sample.

Amino acid analysis of SHPV-B fragments. The amino acid composition of SHPV-B fragments (Pool 2 and Pool 3 in Fig. 4) was determined at the University of Massachusetts Medical Center (Worcester, Massachusetts). Acid hydrolysates were prepared by heating samples in an evacuated bomb containing 5.7 M HCl with 1% phenol at 150 °C for 1.5 h. Pre-column derivatizations with phenyl isothiocyanate were performed by the PICOTAG (Waters Associates, Milford, Massachusetts) procedure and derivatives were separated on a 5-μm PICOTAG reverse-phase column using a Waters HPLC instrument.

Mass spectrometry of the EF fragment. The EF fragment of SHPV-B was purified and lyophilized to a solid powder. The solid was weighed out and solubilized in 5% acetic acid so that the final concentration of the solution was 5 pmol/μL. Solubilized peptide was infused into a Finnigan TSQ 700 instrument with a coaxial sheath flow of 70% MeOH, 0.125% acetic acid, and water, using the conditions described earlier. Mass spectra on the sample were taken using three different modes of operation of the mass spectrometer. The first spectrum was acquired in centroid mode, and the other two were acquired in profile mode, with the last acquisition in profile mode being signal averaged over five scans.

CD of apoSHPV-B, native SHPV-B, and EF fragment. Samples were prepared by dilution of stock solutions of lyophilized protein or peptide, usually in 4 mM HEPES, 100-mM KCl. The final buffer concentration of samples was 2 mM HEPES, 50 mM KCl. Buffered samples ranged from pH 6.2 to 6.8. The apoSHPV-B sample was pH 7.7 and included a 10-fold molar excess of EDTA. For the denatured EF fragment sample, stock solution of EF fragment was dissolved in 3 M guanidine hydrochloride. Protein and peptide concentrations were 25 μM for apoSHPV-B, 21.6 μM for SHPV-B, and 17–150 μM for EF fragment samples. Protein and peptide concentrations of stock solutions were determined by UV absorption using a molar extinction coefficient (E_{1cm}) at 280 nm of 6,970 M^{-1} for native and apoSHPV-B and 5,690 M^{-1} for the EF fragment. Calculation of molar extinction coefficients was based on the method described by Gill and von Hippel (1989). For cation-containing EF fragment samples, a 2:1 molar ratio (cation:peptide) of cation was added to peptide samples using aliquots of 100-mM stock solutions prepared from $CaCl_2$, $TbCl_3$, or, in the case of La^{3+}, a 10-mM stock solution prepared from the hexahydrate of $LaCl_3$.

CD spectra were taken on an AVIV 62DS CD spectrometer at 25 °C unless otherwise indicated. Spectra represent the average of five repeat scans generally recorded between 200 and 300 nm, with readings at 1-nm intervals and an averaging time of 3 s. A 1-mm pathlength rectangular quartz cuvette was used for sample spectra. Using the same cuvette, solvent spectra were recorded and subtracted from sample spectra. The α-helical content of samples was estimated using the methods of Greenfield and Fasman (1969) and Chen et al. (1974). An average of the values obtained by these methods was calculated. For the Chen method, the average length of a helical chain (n) was estimated at 12, based on crystallography data for the EF region of carp (pI 4.25) parvalbumin (Kretsinger & Nockolds, 1973; Kumar et al., 1990).

NMR spectroscopy of EF fragment of SHPV-B. A 4.4-mM sample of EF fragment was prepared by addition of 11.6 mg of peptide to 800 μL 10% D_2O/90% H_2O. One- and two-dimensional NMR

spectra were taken as described above. A twofold molar excess of Ca^{2+} was added to this solution and the 1D and 2D NMR experiments repeated. Before spectral analysis, samples were adjusted to pH 6.4 to 6.5 using 0.2 M NaOH.

Two-dimensional ^1H NMR spectra were acquired at 25 °C. Water suppression was achieved by presaturation during the delay period or mixing time. Two-dimensional spectra were recorded using 2K data points and a spectral width of 6,500 Hz. TOCSY spectra were acquired with 32–96 transients, 256 increments, and an 80-ms mixing time. NOESY spectra were recorded using 48–64 transients, 256 increments, and a mixing time of 150 ms.

From an aliquot of 4.4-mM EF fragment with 2:1 molar ratio of Ca^{2+}, a 2.0-mM EF fragment with 2:1 molar ratio of Ca^{2+} and La^{3+} in 10% D_2O, 90% H_2O, 100 mM NaCl, pH 6.06 was prepared. One-dimensional and TOCSY ^1H NMR spectra were acquired as described previously. A NOESY was recorded using parameters described previously, except that a mixing time of 250 ms was used and water suppression was accomplished by replacement of the observation pulse with a jump return as described in Plateau and Gueron (1982).

The concentration dependence and stoichiometric nature of changes observed in the NMR spectrum of the EF fragment following addition of Ca^{2+} were examined by fragment dilution and Ca^{2+} titration experiments. At concentrations above 0.1 mM, peptide association is likely to occur (Shaw et al., 1991a). Dilution experiments are a classic method of detecting bimolecular processes such as aggregation. In the dilution experiment, the 4.4-mM EF fragment solution (in 10% D_2O, 90% H_2O, pH 6.4, with a twofold molar excess of Ca^{2+}) described above was subjected to successive dilutions and a 1D ^1H NMR spectrum of each diluted sample was taken as described previously. Dilutions were made by addition of 400 μL of D_2O to 400 μL of sample (e.g., 4.4 mM solution was diluted to 2.2 mM; 2.2 mM solution was diluted to 1.1 mM, etc.). Six dilutions were made, resulting in a final sample concentration of 0.07 mM. For more dilute fragment solutions, 1,024 scans were acquired.

To study the reversibility of Ca^{2+}-induced chemical shift changes in the 1D ^1H NMR spectrum of the EF fragment, Ca^{2+} was extracted from a 0.55-mM EF fragment sample using a 10-fold molar excess of EDTA. The pH of this sample was adjusted to 7.5 using 0.2 M NaOH and 0.2 M HCl. A 1D ^1H NMR spectrum was taken as described previously.

The effect of metal ion concentration on EF fragment structure was examined by titration of EF fragment with La^{3+} or Ca^{2+} and observation of the resulting changes in the methyl region of the 1D ^1H NMR spectrum. A 2.8-mM solution of EF fragment (100% D_2O, pH 6.5) containing an internal standard of 3-(trimethylsilyl) propionic-2,2,3,3-d_4 acid sodium salt was prepared and a 1D ^1H NMR spectrum taken. To this sample, Ca^{2+} was added in increments of 0.25 or greater molar equivalents (Ca^{2+}:peptide) by addition of aliquots of 0.25 M $CaCl_2$ in D_2O. Following addition of each aliquot, the sample was agitated, incubated for 15 min, and a 1D ^1H NMR spectrum was taken as described previously using 256 transients. Spectra were acquired for samples in which the molar ratio of Ca^{2+} to peptide varied from 0 to 20. The above experiment was repeated with La^{3+} using 2.6 mM EF fragment (100% D_2O, pH 6.7) and 0.2 or 0.5 molar equivalent additions of La^{3+}. The ratio of La^{3+}:EF fragment ranged from 0 to 1.6.

Sedimentation equilibrium analysis of EF fragment of SHPV-B. The z-average molecular weights of SHPV-B with bound Ca^{2+} were determined by short-column sedimentation equilibrium in 10 mM PIPES, pH 6.5, at peptide concentrations of 0.19–1.5 mg/mL using charcoal-filled Epon centerpieces and the interference optical system of the Beckman XLI ultracentrifuge. To explore the association behavior of the EF fragment of SHPV-B, data were acquired in 10 mM PIPES, pH 6.5, using 3-mm, high-speed centerpieces, absorbance optics at 280 nm from cell, and cell loading concentrations of 1.0, 0.8, 0.5, 0.35 mg/mL. For both types of experiments, concentration distributions were acquired at rotor speeds of 30,000, 40,000, and 45,000 rpm at 20 °C. Equilibrium was demonstrated by showing no change in the concentration distributions for scans taken an hour apart. Data were interpreted using a calculated partial specific volume of 0.7369 mL/g and a calculated molar extinction coefficient of 5,500/cm-M at 280 nm.

Acknowledgments

We thank Bob Talanian of BASF Bioresearch Corp. (Worcester, Massachusetts) for use of the CD spectrometer, Robert Caraway of the Protein Analysis Facility, University of Massachusetts Medical Center (Worcester, Massachusetts) for performing the amino acid composition analyses of the SHPV-B fragments, Dale Mierke for valuable discussions on NMR techniques, Nancy King for collaboration on isoelectric focusing experiments, and Wendy Li for helpful discussions on native SHPV-B. This work was supported by an NIH grant (GM 37537) to D.F.H. and NSF grant (BIR 9314040) to T.M.L.

References

Altschul SF, Gish W, Miller W, Myers EW, Lipman DJ. 1990. Basic local alignment search tool. *J Mol Biol 215*:403–410.

Benzonana G, Capony JP, Pechère JF. 1972. Binding of calcium to muscular parvalbumin. *Biochim Biophys Acta 278*:110–116.

Borin G, Pezzoli A, Marchiori F, Peggion E. 1985. Synthetic and binding studies on the calcium binding site I of bovine brain calmodulin. *Int J Peptide Protein Res 30*:613–622.

Capony JP, Ryden L, Demaille J, Pechère JF. 1973. The primary structure of the major parvalbumin from hake muscle. Overlapping peptides obtained with chemical and enzymatic methods. The complete amino-acid sequence. *Eur J Biochem 32*:97–108.

Chen YH, Yang JT, Chau KH. 1974. Determination of the helix and β form of proteins in aqueous solution by circular dichroism. *Biochemistry 13*:3350–3359.

Coffee CJ, Bradshaw RA. 1973. Carp muscle calcium-binding protein. I. Characterization of the tryptic peptides and the complete amino acid sequence of component B. *J Biol Chem 248*:3305–3312.

Cox J, Milos M, McManus JP. 1990. Calcium- and magnesium-binding properties of oncomodulin. *J Biol Chem 265*:6633–6637.

Declercq JP, Tinant B, Parello J, Rambaud J. 1991. Ionic interactions with parvalbumins. Crystal structure determination of pike 4.10 parvalbumin in four different ionic environments. *J Mol Biol 220*:1017–1039.

Derancourt J, Haiech J, Pechère JF. 1978. Binding of calcium by parvalbumin fragments. *Biochim Biophys Acta 532*:373–375.

Drabikowski W, Brzeska H, Venyaminov SY. 1982. Tryptic fragments of calmodulin: Ca^{2+} and Mg^{2+}-induced conformational changes. *J Biol Chem 257*:11584–11590.

Drake SK, Falke JJ. 1996. Kinetic tuning of the EF-hand calcium binding motif: The gateway residue independently adjusts (i) barrier height and (ii) equilibrium. *Biochemistry 35*:1753–1760.

Drakenberg T, Swärd M, Cavé A, Parello J. 1985. Metal-ion binding to parvalbumin. A ^{113}Cd-n.m.r. study of the binding of different lanthanide ions. *Biochem J 227*:711–717.

Durussel I, Luan-Rilliet Y, Petrova T, Takagi T, Cox JA. 1993. Cation binding and conformation of tryptic fragments of *Nereis* sarcoplasmic calcium-binding protein: Calcium-induced homo- and heterodimerization. *Biochemistry 32*:2394–2400.

Eberspach I, Strassburger W, Glatter U, Gerday C, Wollmer A. 1988. Interaction of parvalbumin of pike II with calcium and terbium ions. *Biochim Biophys Acta 952*:67–76.

Elsayed S, Bennich H. 1975. The primary structure of allergen M from cod. *Scandinavian J Immunol 4*:203–208.

Falke JJ, Drake SK, Hazard AL, Peersen OB. 1994. Molecular tuning of ion binding to calcium signaling proteins. *Q Rev Biophys 27*:219–290.

Filimonov VV, Pfeil W, Tsalkova TN, Privalov P. 1978. *Biophys Chem 8*:117–122.

Finn BE, Kördel J, Thulin E, Sellers P, Forsén S. 1992. Dissection of calbindin D_{9k} into two Ca^{2+}-binding subdomains by a combination of mutagenesis and chemical cleavage. *FEBS Lett 298*:211–214.

Gariépy J, Kay LE, Kuntz ID, Sykes BD, Hodges RS. 1985. Nuclear magnetic resonance determination of metal–proton distances in a calcium binding site of rabbit skeletal troponin C. *Biochemistry 24*:544–550.

Gariépy J, Sykes BD, Hodges RS. 1983. Lanthanide-induced peptide folding: Variations in lanthanide affinity and induced peptide conformation. *Biochemistry 22*:1765–1772.

Gariépy J, Sykes BD, Reid RE, Hodges RS. 1982. Proton nuclear magnetic resonance investigation of synthetic calcium-binding peptides. *Biochemistry 21*:1506–1512.

George SE, Su Z, Fan D, Means AR. 1993. Calmodulin–cardiac troponin C chimeras. *J Biol Chem 268*:25213–25220.

Gerday C. 1976. The primary structure of the parvalbumin II of pike (*Esox lucius*). *Eur J Biochem 70*:305–318.

Gill SC, von Hippel PH. 1989. Calculation of protein extinction coefficients from amino acid sequence data. *Anal Biochem 182*:319–326.

Gilles AM, Imhoff JM, Keil B. 1979. α-Clostripain: Chemical characterization, activity and thiol content of the highly active form of clostripain. *J Biol Chem 254*:1462–1468.

Greenfield N, Fasman GD. 1969. Computed circular dichroism spectra for the evaluation of protein conformation. *Biochemistry 8*:4108–4115.

Hutnik CML, MacManus JP, Szabo AG. 1990. A calcium-specific conformational response of parvalbumin. *Biochemistry 29*:7318–7328.

Joassin L, Gerday C. 1977. The amino acid sequence of the major parvalbumin of the whiting. *Comp Biochem Physiol B Biochem Mol Biol 57*:159–161.

Kawasaki H, Kretsinger RH. 1994. Calcium-binding proteins 1: EF-hands 1:4. London, UK: Academic Press.

Kay LE, Forman-Kay JD, McCubbin WD, Kay CM. 1991. Solution structure of a polypeptide dimer comprising the fourth Ca^{2+}-binding site of troponin C by nuclear magnetic resonance spectroscopy. *Biochemistry 30*:4323–4333.

Kippen AD, Sancho J, Fersht AR. 1994. Folding of barnase in parts. *Biochemistry 33*:3778–3786.

Kretsinger RH. 1972. Gene triplication deduced from the terniary structure of a muscle calcium binding protein. *Nature New Biol 240*:85–88.

Kretsinger RH. 1975. Hypothesis: Calcium modulated proteins contain EF-hands. In: Carafoli E, ed. *Calcium transport in contraction and secretion*. Amsterdam: North-Holland Publishing. p 469.

Kretsinger RH. 1980. Structure and evolution of calcium-modulated proteins. *CRC Crit Rev Biochem 8*:119–174.

Kretsinger RH, Nelson DJ. 1976. Calcium in biological systems. *Coordination Chemistry Reviews 18*:29–124.

Kretsinger RH, Nockolds CE. 1973. Carp muscle calcium-binding protein. *J Biol Chem* 248:3313–3326.

Kumar VD, Lee L, Edwards BFP. 1990. Refined crystal structure of calcium-liganded carp parvalbumin 4.25 at 1.5-Å resolution. *Biochemistry 29*:1404–1412.

Leavis PC, Rosenfeld SS, Gergely J, Grabarek Z, Drabikowski W. 1978. Proteolytic fragments of troponin C. Localization of high and low affinity Ca^{2+} binding sites and interactions with troponin I and troponin T. *J Biol Chem 253*:5452–5459.

Lee L, Corson DC, Sykes BD. 1985. Structural studies of calcium-binding proteins using nuclear magnetic resonance. *Biophys J 47*:139–142.

Lee L, Sykes BD. 1983. Use of lanthanide-induced nuclear magnetic resonance shifts for determination of protein structure in solution: EF calcium binding site of carp parvalbumin. *Biochemistry 22*:4366–4373.

Linse S, Thulin E, Sellers P. 1993. Disulfide bonds in homo- and heterodimers of EF-hand subdomains of calbindin D_{9k}: Stability, calcium binding and NMR studies. *Protein Sci 2*:985–1000.

Miller TL, Cook RM, Nelson DJ, Theoharides AD. 1980. Terbium luminescence from the calcium binding sites of parvalbumin. *J Mol Biol 141*:223–226.

Mitchell WM, Harrington WF. 1968. Purification and properties of clostridiopeptidase B (clostripain). *J Biol Chem 243*:4683–4692.

Monera OD, Shaw GS, Zhu BY, Sykes BD, Kay CM, Hodges RS. 1992. Role of interchain α-helical hydrophobic interactions in Ca^{2+} affinity, formation and stability of a two-site domain in troponin C. *Protein Sci 1*:945–955.

Nelson DJ, Miller TL, Martin RB. 1977. Non-cooperative Ca (II) removal and Terbium (III) substitution in carp muscle calcium binding parvalbumin. *Bioinorganic Chem 7*:325–334.

Padilla A, Cave A, Parello JJ. 1988. Two-dimensional ^1H nuclear magnetic resonance study of pike pI 5.0 parvalbumin (*Esox lucius*). *Mol Biol 204*:995–1017.

Pechère JF, Demaille J, Capony JP. 1971. Muscular parvalbumins: Preparative and analytical methods of general applicability. *Biochim Biophys Acta 236*:391–408.

Permyakov EA, Medvedkin VN, Mitin YV, Kretsinger RH. 1991. Noncovalent complex between domain AB and domains CD*EF of parvalbumin. *Biochim Biophys Acta 1076*:67–70.

Plateau P, Gueron M. 1982. Exchangeable proton NMR without base-line distortion, using new strong-pulse sequences. *J Am Chem Soc 104*:7310–7311.

Prat Gay Gde, Fersht AR. 1994. Generation of a family of protein fragments for structure-folding studies. 1. Folding complementation of two fragments of chymotrypsin inhibitor-2 formed by cleavage at its unique methionine residue. *Biochemistry 33*:7957–7963.

Prat Gay Gde, Ruiz-Sanz J, Fersht AR. 1994. Generation of a family of protein fragments for structure-folding studies. 2. Kinetics of association of the two chymotrypsin inhibitor-2 fragments. *Biochemistry 33*:7964–7970.

Ragg E, Cavé A, Drakenberg T. 1986. Metal ion binding to parvalbumin. A proton NMR study. *Acta Chem Scand 40*:6–14.

Reid RE. 1990. Synthetic fragments of calmodulin calcium-binding site III. *J Biol Chem 265*:5971–5976.

Reid RE, Gariépy J, Saund AK, Hodges RS. 1981. Calcium-induced protein folding. *J Biol Chem 256*:2742–2751.

Renner M, Danielson MA, Falke JJ. 1993. Kinetic control of Ca (II) signaling: Tuning the ion dissociation rates of EF-hand Ca (II) binding sites. *Proc Natl Acad Sci USA 90*:6493–6497.

Rico M, Jiménez MA, Gonzáles C, De Filippis V, Fontana A. 1994. NMR solution structure of the c-terminal fragment 255–316 of thermolysin: A dimer formed by subunits having the native structure. *Biochemistry 33*:14834–14847.

Roongta V, Powers R, Jones C, Beakage MJ, Shields JE, Gorenstein DG. 1989. Solution conformation of a synthetic fragment of human pituitary growth hormone. Two-dimensional NMR of an α-helical dimer. *Biochemistry 28*:1048–1054.

Shaw GS, Findlay WA, Semchuk PD, Hodges RS, Sykes BD. 1992a. Specific formation of a heterodimeric two-site calcium-binding domain from synthetic peptides. *J Am Chem Soc 114*:6258–6259.

Shaw GS, Golden LF, Hodges RS, Sykes BD. 1991a. Interactions between paired calcium-binding sites in proteins: NMR determination of the stoichiometry of calcium binding to a synthetic troponin-C peptide. *J Am Chem Soc 113*:5557–5563.

Shaw GS, Hodges RS, Kay CM, Sykes BD. 1994. Relative stabilities of synthetic peptide homo- and heterodimeric troponin-C domains. *Protein Sci 3*:1010–1019.

Shaw GS, Hodges RS, Sykes BD. 1990. Calcium-induced peptide association to form an intact protein domain: ^1H NMR structural evidence. *Science 249*:280–283.

Shaw GS, Hodges RS, Sykes BD. 1991b. Probing the relationship between α-helix formation and calcium affinity in troponin C: ^1H NMR studies of calcium binding to synthetic and variant site III helix-loop-helix peptides. *Biochemistry 30*:8339–8347.

Shaw GS, Hodges RS, Sykes BD. 1992b. Determination of the solution structure of a synthetic two-site calcium-binding homodimeric protein domain by NMR spectroscopy. *Biochemistry 31*:9572–9580.

Shaw GS, Hodges RS, Sykes BD. 1992c. Stoichiometry of calcium binding to a synthetic heterodimeric troponin C domain. *Biopolymers 32*:391–397.

Shaw GS, Sykes BD. 1996. NMR solution structure of a synthetic troponin C heterodimeric domain. *Biochemistry 35*:7429–7438.

Shoemaker KR, Fairman R, Kim PS, York EJ, Stewart JM, Baldwin RL. 1987. The C-peptide helix from ribonuclease A considered as an autonomous folding unit. *Cold Spring Harbor Symp Quant Biol 52*:391–398.

Struthers MD, Cheng RP, Imperiali B. 1996. Design of a monomeric 23-residue polypeptide with defined tertiary structure. *Science 171*:342–345.

Strynadka NC, James MNG. 1989. Crystal structures of the helix-loop-helix calcium-binding proteins. *Annu Rev Biochem 58*:951–998.

Tsalkova TN, Privalov PL. 1985. Thermodynamic study of domain organization in troponin C and calmodulin. *J Mol Biol 181*:533–544.

Tsuji T, Kaiser ET. 1991. Design and synthesis of the pseudo-EF hand in calbindin D_{9k}: Effect of amino acid substitutions in the α-helical regions. *Proteins Struct Funct Genet 9*:12–22.

Williams J, Moreton K. 1988. The dimerization of half-molecule fragments of transferrin. *Biochem J 251*:849–855.

Williams TC, Corson DC, Oikawa K, McCubbin WD, Kay CM, Sykes BD. 1986. ^1H NMR studies of calcium-binding proteins. 3. Solution conformations of rat apo-α-parvalbumin and metal-bound rat α-parvalbumin. *Biochemistry 29*:1829–1840.

Zhang C, Nelson DJ. 1992. ^{113}Cd Nuclear magnetic resonance study of the binding of Cd^{2+} and Lu^{3+} to silver hake parvalbumin. *J Alloys and Compounds 180*:349–356.

Zhang C, Speno H, Clairmont C, Nelson DJ. 1990. The isolation of an unusual parvalbumin from the white muscle of the silver hake, *Merluccius bilinearis*. *J Inorg Biochem 40*:59–79.